NANO LETTERS

Letter

pubs.acs.org/NanoLett

Substrate Stiffness Regulates Cellular Uptake of Nanoparticles

Changjin Huang,[†] Peter J. Butler,[‡] Sheng Tong,[§] Hari S. Muddana,[‡,∥] Gang Bao,[§] and Sulin Zhang*[,†]

[†]Department of Engineering Science and Mechanics and [‡]Department of Bioengineering, The Pennsylvania State University, University Park, Pennsylvania 16802, United States

[§]Department of Biomedical Engineering, Georgia Institute of Technology and Emory University, Atlanta, Georgia 30332, United States

Supporting Information

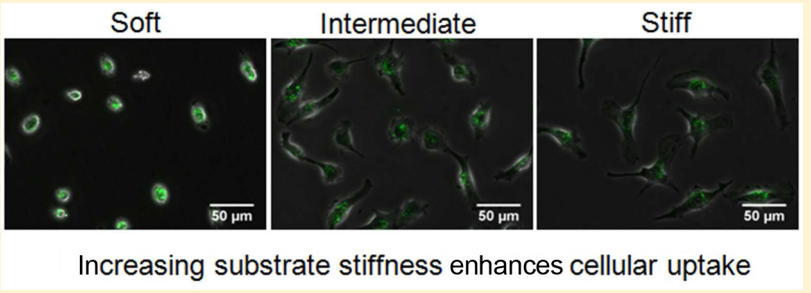

ABSTRACT: Nanoparticle (NP)-bioconjugates hold great promise for more sensitive disease diagnosis and more effective anticancer drug delivery compared with existing approaches. A critical aspect in both applications is cellular internalization of NPs, which is influenced by NP properties and cell surface mechanics. Despite considerable progress in optimization of the NP-bioconjugates for improved targeting, the role of substrate stiffness on cellular uptake has not been investigated. Using polyacrylamide (PA) hydrogels as model substrates with tunable stiffness, we quantified the relationship between substrate stiffness and cellular uptake of fluorescent NPs by bovine aortic endothelial cells (BAECs). We found that a stiffer substrate results in a higher total cellular uptake on a per cell basis, but a lower uptake per unit membrane area. To obtain a mechanistic understanding of the cellular uptake behavior, we developed a thermodynamic model that predicts that membrane spreading area and cell membrane tension are two key factors controlling cellular uptake of NPs, both of which are modulated by substrate stiffness. Our experimental and modeling results not only open up new avenues for engineering NP-based cancer cell targets for more effective in vivo delivery but also contribute an example of how the physical environment dictates cellular behavior and function.

KEYWORDS: *Substrate stiffness, cellular uptake, nanoparticles, cellular spreading, membrane tension, cancer therapy*

The past decade has witnessed rapid progress in the design of surface functionalized and bioconjugated nanoparticles (NPs) for highly targeted cancer diagnosis and therapy. In order to optimize cellular uptake of NPs for enhanced diagnostic imaging and/or drug dosage in diseased organs, in vitro experiments[1−3] and thermodynamic[4−7] and kinetic[8,9] analyses have been conducted to elucidate how the size, shape, and surface chemistry of NPs affect endocytosis-mediated cellular uptake. However, to date there have been no studies aimed at elucidating the role of local physical environments on endocytosis of NPs despite the widely known effect of extracellular matrix (ECM) mechanics on cellular responses and disease states in vivo. Advances in mechanobiology have established that mechanical cues modulate many cell responses, though such modulation is cell-type dependent. In particular, substrate stiffness has been shown to be a regulatory factor for cell spreading,[10] locomotion,[11−13] differentiation,[14−16] and proliferation.[17] It is possible, therefore, that stiffness-regulated cell responses also modulate NP uptake kinetics, and this phenomenon could be utilized as a new avenue to optimize NP designs for more effective in vivo delivery.

The studies of the effect of substrate stiffness on cellular uptake of NPs have other significant implications. In relevant physiological conditions, tumor tissues have different stiffnesses as they go through different stages.[18] In addition, a metastatic cancer cell migrates along tissues of varying stiffness.[19] If the mechanical properties of ECM indeed mediate cellular uptake, such an effect should be taken into account in the optimization of NP-based cancer cell targeting for inhibiting tumor growth and cancer cell metastasis. Though much is known separately about cell responses to their local physical environments and the size/shape dependent cellular uptake of NPs, the effect of ECM stiffness on cellular uptake, despite its high clinical and biological relevance, remains unexplored.

Received: January 4, 2013
Revised: March 7, 2013

   dx.doi.org/10.1021/nl400033h | *Nano Lett.* XXXX, XXX, XXX−XXX

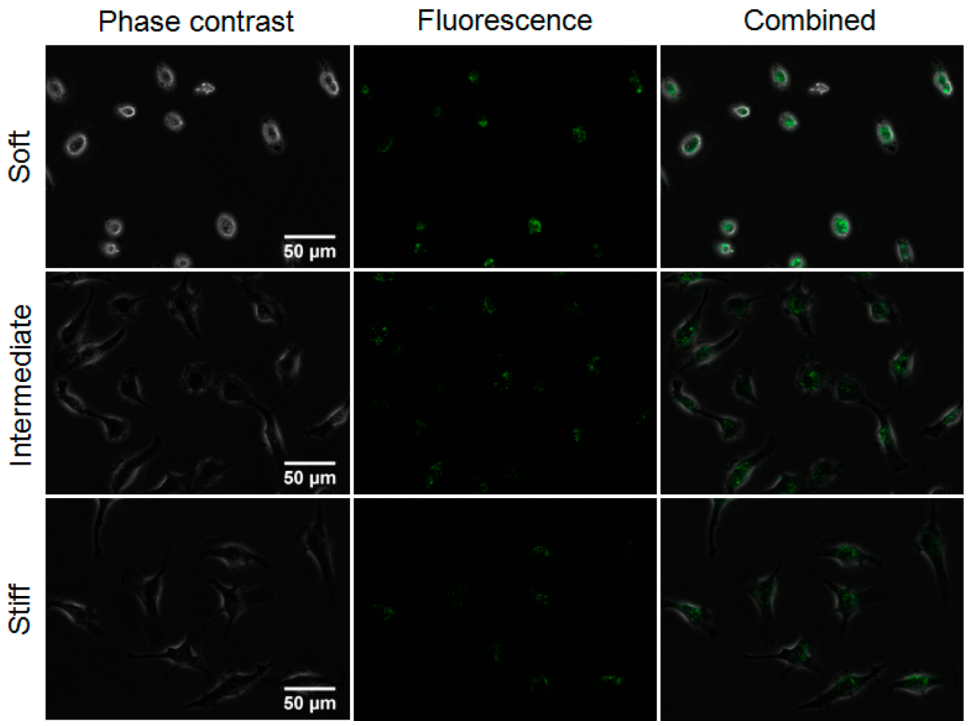

Figure 1. Cellular uptake of fluorescent NPs by the cells on PA substrates of varying stiffness. Cells were cultured on substrates for 12 h before loading the NPs. Images were taken after loading the NPs for 6 h.

While the substrates on which cells are cultured in vitro, commonly glass or plastic materials coated with biomolecules (e.g., fibronectin), can mimic the biochemical interactions between cells and ECM in vivo, their stiffness is usually several orders of magnitude different from that of ECM in vivo. Herein, we report, using PA hydrogels of varying stiffness as model substrates and fluorescent polystyrene NPs, that the total cellular uptake of NPs by BAECs increases with increasing gel stiffness. To gain insight into the underlying mechanisms, we characterized the relationship between substrate stiffness, spreading area, apical stress fiber formation, and apical membrane tension. By measuring fluorescence lifetime of a lipophilic dye using time-correlated single photon counting (TCSPC), we deduced that increasing substrate stiffness leads to increased membrane tension. The increased tension correlates with increased apical actin fiber formation, as confirmed by confocal microscopy imaging. A thermodynamics model complementary to the experimental characterization was then established to rationalize the role of substrate stiffness on the cellular uptake. The model predicts that cell membrane surface area and membrane tension are the governing factors that dictate the cellular uptake of NPs, both of which are modulated by the substrate stiffness. The findings provide new insight into the rational design of NP-based therapeutic and diagnostic agents for disease detection and treatment.

The following three groups of PA gel substrates were prepared: soft (8% acrylamide/0.02% bis-acrylamide), intermediate (8% acrylamide/0.05% bis-acrylamide), and stiff (8% acrylamide/0.08% bis-acrylamide). The Young's moduli of the three gels were measured via indentation experiments using an atomic force microscope (AFM) and found to be 1.61 ± 0.11 kPa (soft), 3.81 ± 0.12 kPa (intermediate), and 5.71 ± 0.51 kPa (stiff), respectively, all of which fall within the physiological range of biological tissues.[15] We chose the stiffness of this range since the cell line (BAECs) used in our experiments is mostly sensitive to this range, as suggested by the previous studies.[10] To facilitate cell adhesion, the gels were surface-coated with fibronectin bridged via Sulfo-SANPAH. The density of fibronectin on the PA gel surface is independent of the gel stiffness, as reported in previous studies.[10,20]

BAECs were cultured on PA gel substrates for 12 h before loading NPs into the culture media. Phase contrast images clearly show that the gel stiffness modulates cell morphology (Figure 1). Cells on soft substrates rounded up, while cells on intermediate and stiff substrates were much more spread. Cells on intermediate substrates exhibited relatively smaller size compared to those on stiff substrates. This qualitative observation agrees well with the previous reports by Yeung et al.[10] We further measured the projected spreading area of the cells at certain specified time points upon loading the NPs. The results showed that cell spreading areas remained nearly unchanged after the initial 12 h incubation (Figure 2). These areas were 276.0 ± 58.1, 1025.1 ± 272.7, and 1453.9 ± 266.7 μm^2, for soft, intermediate, and stiff substrates, respectively. It should be pointed out that the total apical cell surface areas might be underestimated by the projected area since cells have a nonzero thickness, especially for the cells grown on soft substrates. The cells grown on soft substrates are around 1.5-fold thicker than those on the intermediate and stiff substrates, while the thickness difference between cells on intermediate and stiff substrates is hardly differentiable from their confocal stacks. Treating the round cells as hemispherical, the cells on soft substrates have a maximum apical cell surface area of 562.3 ± 141.3 μm^2, which is still considerably smaller than the others.

We also examined the influence of gel stiffness on the stress fiber formation in the cells by staining F-actin with phalloidin. Figure 3 shows representative maximal intensity z-projections of F-actin distribution within the cells and corresponding F-actin distribution near the apical surface of the cells on the PA gel substrates. Stress fibers were absent in the round cells on

dx.doi.org/10.1021/nl400033h | Nano Lett. XXXX, XXX, XXX−XXX

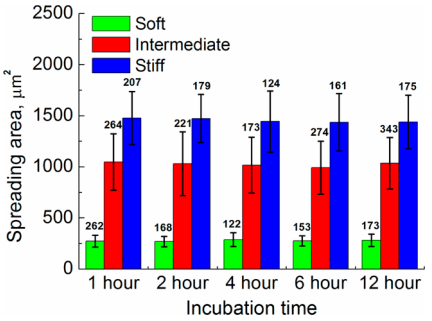

Figure 2. The spreading area of the cells on the PA gels of varying stiffness. Cells were cultured on substrates for 12 h before loading the NPs (the time clock is set to be zero at the time of loading the NPs). The cell spreading reached a steady-state level after 12 h incubation ($p > 0.16$ for all the three types of substrates using the single-factor ANOVA test). The difference in the spreading area between any two groups at each time point of measurement is statistically significant ($p < 0.01$ using Student t-test). The numbers of cells studied for each group are listed above each corresponding column.

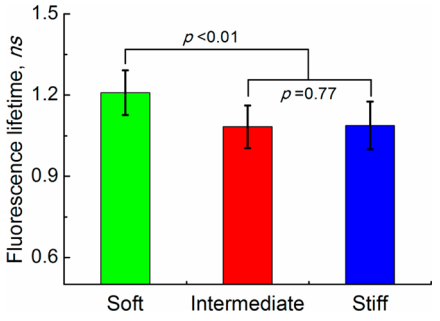

Figure 4. Fluorescence lifetime of DiI-C_{12} in apical membranes of the cells grown on PA gels of varying stiffness (3 repeated experiments, 10 cells/experiment).

soft gels and only discrete bright spots were observed. Cells on stiff gels exhibited much more aligned stress fibers than those on the intermediate gels. These observations are in good agreement with previous studies.[10,21] These features were also evident on the apical surface of the cell where NPs come into contact first (bottom panel in Figure 3). Considering the cell morphologies on substrates of varying stiffness, the results also show a positive correlation between the cell spreading and actin stress fiber formation.

Previous studies suggested a positive correlation of stress fiber formation and cell stiffness,[21,22] yet no direct evidence has been established concerning the relation of stress fiber formation and membrane tension. Conventional approaches to measure cell membrane tension often involve either indenting or tethering cell surface using atomic force microscope[23] or optical tweezer.[24] The applied mechanical stimulation might disturb cell organization and induce cell remodeling.[25,26] Our recent molecular dynamics simulation results suggested that the fluorescence lifetime of DiI chromophores embedded in lipid bilayer is an effective indicator of relative membrane tension,[27] which was later confirmed in experiments.[28] Briefly, membrane tension reduces membrane lipid order and headgroup viscosity, and consequently reduces the DiI fluorescence lifetime. Figure 4 shows the fluorescence lifetime of DiI-C_{12} within cells on PA gels of varying stiffness. The DiI fluorescence lifetime in cells on soft substrates (τ_{soft} = 1.209 ± 0.083 ns) is significantly longer than that on either intermediate (τ_{inter} = 1.083 ± 0.079 ns) or stiff (τ_{stiff} = 1.088 ± 0.088 ns) substrates, indicating that the cell membrane on soft substrates was much less tense. However, no significant difference in fluorescence lifetime was detected between intermediate and stiff substrates.

We used carboxylated polystyrene NPs (PS-COOH) with diameters of 100 nm in our uptake study. The yellow-green fluorescent dye embedded inside the NPs with minimal photobleaching allows us to quantify cellular uptake at any culture time. Assuming that the fluorescence intensity is proportional to the number of fluorescent NPs, the average fluorescence yield per unit area within individual cells indicates the efficiency of cellular uptake of NPs. It should be mentioned that in extracting the fluorescence intensity, the seeded cells were extensively washed using DPBS to remove the NPs adhered to the cell surface. Therefore, the fluorescence intensity accounts only for the internalized NPs, as confirmed by our three-dimensional confocal images (see Figure S1 in Supporting Information). Figure 5a shows that cellular uptake per unit area decreases with the increasing substrate stiffness at all times measured. Compared to the cells on intermediate and stiff gels, round cells on soft gels uptake NPs much more efficiently. It should be pointed out that the fluorescence intensity per unit area is to certain extent overestimated here due to the underestimation to the apical surface area, especially for the cells grown on soft substrates. However, even if we treat the cells grown on soft substrates as hemispherical, in which case the apical surface area is twice as much as the measured projected area, its fluorescence intensity per unit area is still

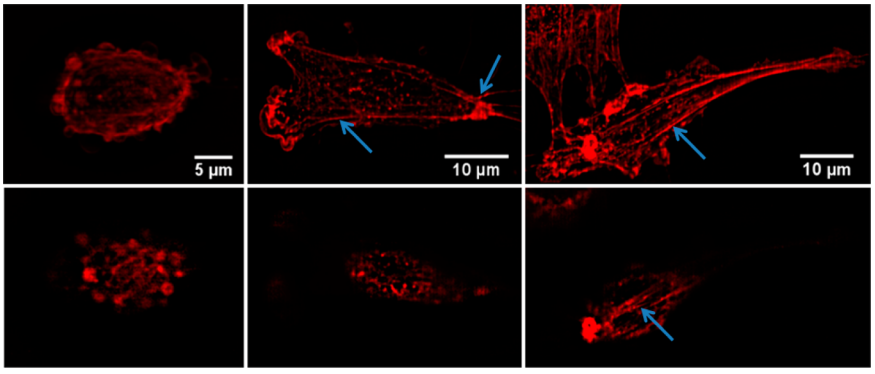

Figure 3. The distribution of F-actin within the cells on the PA gels: soft (left), intermediate (middle), and stiff (right). (Top) maximal intensity z-projections; (bottom) F-actin distribution near the cell apical surface. Arrows in the figure highlight the well-aligned stress fibers.

dx.doi.org/10.1021/nl400033h | Nano Lett. XXXX, XXX, XXX−XXX

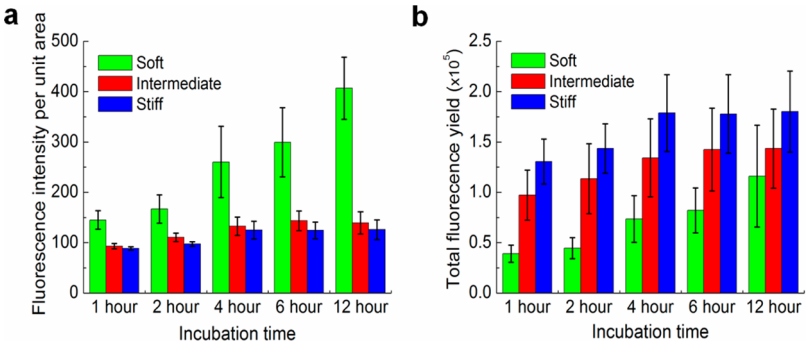

Figure 5. Cellular uptake of NPs on the gels of varying stiffness. (a) The fluorescence yield per unit area of individual cells. (b) The total fluorescence yield of individual cells obtained by multiplying fluorescence per unit area by the projected cell area on a cell by cell basis. In both (a.b), the difference between any two groups at any specified time point of measurement is statistically significant ($p < 0.01$ using Student t-test).

higher than that of the cells on intermediate and stiff substrates after 6 h. The uptake level reached a plateau after 4 h for cells on both intermediate and stiff gels, but continued to increase even after 12 h for cells on soft gels. This difference might originate from the distinct membrane tension levels of the cells on gels of varying stiffness. Compared to cells on soft gels, the higher membrane tension of the cells on intermediate and stiff gels resists NPs from entering cells since the uptake involves a higher membrane deformation energy penalty, as detailed next in our theoretical section. Overlaying the phase contrast and fluorescence images shows that the fluorescence signal was concentrated around cell nuclei, but nearly undetectable near the cell protrusions (Figure 1). This clear contrast might be indicative of the role of membrane tension in inhibiting cellular uptake at the cell protrusions, where cell membrane was highly tensed as a consequence of richly developed stress fibers.[29,30]

We further quantified the total fluorescence yield of individual cells on the gels by multiplying the fluorescence intensity per unit area (Figure 5a) by the projected area (Figure 2) on a cell by cell basis. As seen in Figure 5b, the total fluorescence yield in individual cells increases with increasing gel stiffness at all time points measured. Similar to the kinetics of the fluorescence intensity per unit area, the total fluorescence yield of cells on intermediate and stiff gels reached a plateau after 4 h but not for those on soft gels within 12 h. The uptake level by cells on soft gels might surpass that by cells on intermediate and stiff substrates after prolonged incubation time. However, since NPs usually are cleared out within several hours after intravenous injection,[31] the uptake level after 12 h has little clinical implication and thus is beyond the scope of our study.

Since the NPs used in our experiments were free of surface conjugation with ligand molecules, it is likely that endocytosis occurred in a nonspecific manner. From an energetic point of view, NP internalization is driven by nonspecific adhesion energy but penalized by membrane bending and tension energies. To arrive at a generalized understanding of the cellular uptake behavior, we next perform thermodynamic analyses of the parametric dependence of NP uptake on membrane area and cell surface mechanics and compare these model results with the experimental data. We simplify the experimental settings by considering a cell with a surface area M, bending modulus κ, and membrane tension σ immersed in a solution with dispersed NPs of surface area A_0 and bulk density φ. Here the membrane tension includes the contributions from both the plasma membrane and the cortical layer underneath the membrane. We denote the number of NPs with a wrapped area A as n_A. Through a thermodynamic analysis (see Supporting Information for detailed derivation), the wrapping-size distribution of NPs upon the NP-cell system reaches a steady state can be written as

$$n_A = M\varphi \exp(\mu A - w_A) \quad (1)$$

where μ is the nonspecific adhesion energy density and w_A is the associated membrane deformation energy (including both bending and tension energies) when an NP is wrapped by an area of A. The NPs are fully wrapped and endocytosed when $A = A_0$ at which $w_A = \sigma A_0 + 8\kappa\pi$. Therefore, the total cellular uptake N can be written as

$$N = M\varphi \exp[A_0(\mu - \sigma) - 8\kappa\pi] \quad (2)$$

The cellular uptake per cell surface area is

$$\frac{N}{M} = \varphi \exp[A_0(\mu - \sigma) - 8\kappa\pi] \quad (3)$$

Equations 2 and 3 provide the basis for the comparison with the in vitro experimental data. Similar formula has been derived for receptor-mediated cellular uptake of NPs,[4,5] and the predictions agree reasonably well with corresponding experimental data.[1,32,33] From eq 2, the total cellular uptake increases linearly with increasing cell surface area, but decreases exponentially with increasing membrane tension, assuming that the membrane bending modulus κ remains a constant. The theoretical predictions support our experimental data in that NP uptake increases with increasing area (Figure 5b and eq 2), and decreases with increasing membrane tension (Figure 5a and eq 3).

We conclude by noting that substrate stiffness regulated cellular uptake originates from mechanotransduction of cells. As it has been well established, cells of many different types sense physical cues and respond by emanating a series of biochemical signals that modulates cell spreading, cytoskeletal remodeling, and morphological evolution. Though membrane mechanics modifications due to the change of substrate stiffness need to be further quantified, the present work reports the first experimental evidence regarding how local physical environment regulates cellular uptake of NPs and provides an example of exploiting mechanotransduction in nanomedicine. Considering the dynamically changing physical environments that cells may encounter, for instance, in tumor tissues during different growth stages and in different organs over which metastatic cancer cells migrate, our fundamental understanding of the regulatory role played by the substrate stiffness opens up a new

dx.doi.org/10.1021/nl400033h | Nano Lett. XXXX, XXX, XXX−XXX

dimension to NP optimization for enhanced chemotherapeutic effects and amplified diagnostic signals.

■ ASSOCIATED CONTENT

Supporting Information

Experimental methods and detailed thermodynamical analysis are provided. This material is available free of charge via the Internet at http://pubs.acs.org.

■ AUTHOR INFORMATION

Corresponding Author

*E-mail: suz10@psu.edu.

Present Address

[‖]Skaggs School of Pharmacy and Pharmaceutical Sciences, University of California San Diego, La Jolla, CA 92093.

Notes

The authors declare no competing financial interest.

■ ACKNOWLEDGMENTS

We are grateful to Dr. Lichong Xu at Professor Christopher A. Siedlecki's laboratory in The Pennsylvania State University for his help on AFM measurement of the gel stiffness. S.L.Z. acknowledges the supports in part from National Science Foundation (CMMI-0754463; CBET-1067523). P.J.B. acknowledges the support in part from the National Heart Lung and Blood Institute (R01 HL 07754201-A1) and the National Science Foundation (BES 0238910). G.B. acknowledges supports from the National Institutes of Health as an NHLBI Program of Excellence in Nanotechnology Award (HHSN268201000043C to GB), and the National Science Foundation as a Science and Technology Center grant (CBET-0939511 to GB).

■ REFERENCES

(1) Chithrani, B. D.; Ghazani, A. A.; Chan, W. C. W. *Nano Lett.* **2006**, *6* (4), 662−668.

(2) Jiang, W.; Kim, B. Y. S.; Rutka, J. T.; Chan, W. C. W. *Nat. Nanotechnol.* **2008**, *3* (3), 145−150.

(3) Gratton, S. E. A.; Ropp, P. A.; Pohlhaus, P. D.; Luft, J. C.; Madden, V. J.; Napier, M. E.; DeSimone, J. M. *Proc. Natl. Acad. Sci. U.S.A.* **2008**, *105* (33), 11613−11618.

(4) Zhang, S.; Li, J.; Lykotrafitis, G.; Bao, G.; Suresh, S. *Adv. Mater.* **2009**, *21*, 419−424.

(5) Yuan, H. Y.; Zhang, S. L. *Appl. Phys. Lett.* **2010**, *96* (3), 033704.

(6) Yuan, H. Y.; Li, J.; Bao, G.; Zhang, S. L. *Phys. Rev. Lett.* **2010**, *105* (13), 138101−138104.

(7) Yuan, H. Y.; Huang, C. J.; Zhang, S. L. *PLoS One* **2010**, *5* (10), e13495.

(8) Gao, H. J.; Shi, W. D.; Freund, L. B. *Proc. Natl. Acad. Sci. U.S.A.* **2005**, *102* (27), 9469−9474.

(9) Bao, G.; Bao, X. R. *Proc. Natl. Acad. Sci. U.S.A.* **2005**, *102* (29), 9997−9998.

(10) Yeung, T.; Georges, P. C.; Flanagan, L. A.; Marg, B.; Ortiz, M.; Funaki, M.; Zahir, N.; Ming, W. Y.; Weaver, V.; Janmey, P. A. *Cell Mobil. Cytoskel.* **2005**, *60* (1), 24−34.

(11) Lo, C. M.; Wang, H. B.; Dembo, M.; Wang, Y. L. *Biophys. J.* **2000**, *79* (1), 144−152.

(12) Zaman, M. H.; Trapani, L. M.; Siemeski, A.; MacKellar, D.; Gong, H.; Kamm, R. D.; Wells, A.; Lauffenburger, D. A.; Matsudaira, P. *Proc. Natl. Acad. Sci. U. S. A.* **2006**, *103* (29), 10889−10894.

(13) Tang, X.; Kuhlenschmidt, T. B.; Zhou, J. X.; Bell, P.; Wang, F.; Kuhlenschmidt, M. S.; Saif, T. A. *Biophys. J.* **2010**, *99* (8), 2460−2469.

(14) Discher, D. E.; Janmey, P.; Wang, Y.-l. *Science* **2005**, *310* (5751), 1139−1143.

(15) Engler, A. J.; Sen, S.; Sweeney, H. L.; Discher, D. E. *Cell* **2006**, *126* (4), 677−689.

(16) Wan, C.-r.; Chung, S.; Kamm, R. D. *Ann. Biomed. Eng.* **2011**, *39* (6), 1840−1847.

(17) Tilghman, R. W.; Cowan, C. R.; Mih, J. D.; Koryakina, Y.; Gioeli, D.; Slack-Davis, J. K.; Blackman, B. R.; Tschumperlin, D. J.; Parsons, J. T. *PLoS One* **2010**, *5* (9), 13.

(18) Huang, S.; Ingber, D. E. *Cancer Cell* **2005**, *8* (3), 175−176.

(19) Lee, G. Y. H.; Lim, C. T. *Trends Biotechnol.* **2007**, *25* (3), 111−118.

(20) Tse, J. R.; Engler, A. J. Preparation of Hydrogel Substrates with Tunable Mechanical Properties. In *Current Protocols in Cell Biology*; John Wiley & Sons, Inc.: New York, 2010.

(21) Byfield, F. J.; Reen, R. K.; Shentu, T.-P.; Levitan, I.; Gooch, K. J. *J. Biomech.* **2009**, *42* (8), 1114−1119.

(22) Sassoli, C.; Meacci, E.; Nosi, D.; Squecco, R. *Am. J. Physiol.* **2008**, *295* (1), C160−C172.

(23) Sen, S.; Subramanian, S.; Discher, D. E. *Biophys. J.* **2005**, *89* (5), 3203−3213.

(24) Upadhyaya, A.; Sheetz, M. P. *Biophys. J.* **2004**, *86* (5), 2923−2928.

(25) Mack, P. J.; Kaazempur-Mofrad, M. R.; Karcher, H.; Lee, R. T.; Kamm, R. D. *Am. J. Physiol.* **2004**, *287* (4), C954−C962.

(26) Melzak, K. A.; Lazaro, G. R.; Hernandez-Machado, A.; Pagonabarraga, I.; de Espada, J.; Toca-Herrera, J. L. *Soft Matter* **2012**, *8* (29), 3716−3726.

(27) Muddana, H. S.; Gullapalli, R. R.; Manias, E.; Butler, P. J. *Phys. Chem. Chem. Phys.* **2011**, *13* (4), 1368−1378.

(28) Tabouillot, T.; Muddana, H. S.; Butler, P. J. *Cell. Mol. Bioeng.* **2011**, *4* (2), 169−181.

(29) Tan, J. L.; Tien, J.; Pirone, D. M.; Gray, D. S.; Bhadriraju, K.; Chen, C. S. *Proc. Natl. Acad. Sci. U.S.A.* **2003**, *100* (4), 1484−1489.

(30) Parsons, J. T.; Horwitz, A. R.; Schwartz, M. A. *Nat. Rev. Mol. Cell. Bio.* **2010**, *11* (9), 633−643.

(31) Alexis, F.; Pridgen, E.; Molnar, L. K.; Farokhzad, O. C. *Mol. Pharmaceutics* **2008**, *5* (4), 505−515.

(32) Desai, M. P.; Labhasetwar, V.; Walter, E.; Levy, R. J.; Amidon, G. L. *Pharm. Res.* **1997**, *14* (11), 1568−1573.

(33) Osaki, F.; Kanamori, T.; Sando, S.; Sera, T.; Aoyama, Y. *J. Am. Chem. Soc.* **2004**, *126* (21), 6520−6521.